Scripta Materialia 153 (2018) 23–26

Contents lists available at ScienceDirect

Scripta Materialia

journal homepage: www.elsevier.com/locate/scriptamat

Regular article

Transformation behavior and superelastic properties of Ti-Ni-Ag scaffolds prepared by sintering of alloy fibers

Shuanglei Li [a], Yeon-wook Kim [b], Tae-hyun Nam [a,*]

[a] School of Materials Science and Engineering & RIGET, Gyeongsang National University, 900 Gazwadong, Jinju, Gyeongnam 52828, Republic of Korea
[b] Department of Material Engineering, Keimyung University, 1000 Shindang-dong, Dalseo-gu, Daegu 704-701, Republic of Korea

ARTICLE INFO

Article history:
Received 15 November 2017
Received in revised form 30 January 2018
Accepted 1 February 2018
Available online xxxx

Keywords:
Ti-Ni-Ag alloy
Rapid solidification
Sintering
Porous material
Superelasticity

ABSTRACT

Ti-50.3Ni-0.7Ag (at.%) scaffolds were prepared by sintering of rapidly solidified alloy fibers. The sintered scaffolds possessed high porosity of 80% and large pores of 150–600 μm in size. The yield strength of the scaffold after annealed at 723 K for 3.6 ks was about 2.4 MPa. Ti-Ni-Ag scaffolds had an elastic modulus of 0.8 GPa, similar to that of spongy bone, and exhibited good superelasticity with total recovery strain of 3.4% when 4% pre-strain was loaded at human body temperature. Stable superelastic behavior with complete shape recovery was observed during cyclic deformation in scaffolds.

Ti-Ni alloys are promising implant materials in biomedical fields due to their excellent properties, such as shape memory effect, superelasticity and biocompatibility [1]. In particular, TiNi alloys have similar deformation behavior with that of bone, compared to other metallic materials, which can guarantee the biomechanical compatibility [2]. There has been increased interest in TiNi porous materials for bone implant by reason of the increase in the number of people suffering from osteoporosis, broken bones and skeletal defects due to the increasingly active lifestyle, accidents and ageing population [3,4]. In addition to the superelasticity, porous TiNi shape memory alloys have large potential for biomaterials due to their low density, the ability to support early ingrowth of bone and adjustable elastic modulus [5,6].

Infection diseases are the second most common cause of death worldwide and biomaterials-associated infections have been increasingly recognized as a principle failure mechanism of implanted scaffolds [7]. Therefore, there is an urgent need to develop antibacterial scaffolds for avoiding such infections and catastrophic consequences. Recently, the effect of silver addition into Ti-Ni alloys has attracted researchers' attention because of the antibacterial property of silver [9]. It has been reported that Ag ions can affect the bacterial viability by reacting with tissue proteins of cell membrane [10,11]. Silver addition to TiNi alloys also improved the corrosion resistance because they have a stable passive film [12]. The high corrosion resistance can minimize the adverse effect of nickel release, which is beneficial for biomedical applications when used in the human body. Ti-Ni-Ag alloys exhibiting little or no cytotoxicity not only have excellent biocompatibility but also present antibacterial property and good corrosion resistance [1,12,13]. Thus, the purpose of this study is to fabricate Ti-Ni-Ag scaffolds with antibacterial function and appropriate mechanical properties for replacing damaged bones.

In order to promote tissue growth, the scaffold must have a large surface to allow cell attachment, which is usually done by creating a highly porous structure [14]. Currently, many studies have been carried out to fabricate highly porous scaffolds with superelasticity, which can meet the requirements of bone replacement materials, e.g., 50–90% porosity in cancellous bone [15]. However, only a few studies have achieved the level of porosity above 80% by powder metallurgy [16]. Ti-Ni alloy foams with porosity of 87% were fabricated by space-holder sintering process [5]. However, these foams exhibited a low strength with plateau stress of 1.9 MPa and elastic modulus of 0.03 GPa, which is a big obstacle to practical application. Fiber metallurgy has some advantages over powder metallurgy ones. The possible porosity for fiber metallurgy is much wider, extending from zero to 95%, than powder metallurgy usually extending zero to 60% [17,18]. Porous fiber scaffolds also have higher strength and ductility than porous powder scaffolds at equal porosity [19]. Therefore, porous metallic scaffolds are prepared in this study by sintering of alloy fibers.

Pre-alloy with the nominal composition of 49Ti-50.3Ni-0.7Ag (at.%) was prepared by arc melting and then alloy fibers were produced from pre-ingot by using an arc melt overflow device [20]. As-solidified alloy fibers were cut into small segments with the length about 5 mm and then put into the packing chamber of graphite mold and sintered at 1273 K for 3.6 ks in high vacuum conditions. The sample was cooled

* Corresponding author.
E-mail address: tahynam@gnu.ac.kr (T. Nam).

https://doi.org/10.1016/j.scriptamat.2018.02.003
1359-6462/

in the equipment to room temperature after sintering. After sintering, the scaffold was annealed at 723 K for 3.6 ks in vacuum (10^{-3} Pa), followed by quenching into iced water. In order to investigate transformation temperatures, DSC measurements were made with a cooling and heating rate of 0.17 K s^{-1} by using TA instrument DSC Q20. Crystal structures were studied at various temperatures by X-ray diffraction (XRD, D8 advance) using Cu Kα radiation with a scanning rate of 2°min^{-1}. The compressive tests of scaffold were performed by using shape memory simulator at human body temperature. The size of sample was 8 mm × 8 mm × 10 mm.

Fig. 1(a) shows the morphology of as-spun Ti-Ni-Ag fibers observed by SEM. Continuous fibers were produced and the cross-sectional shape inserted in Fig. 1(a) was close to a circular with average diameter of 90 μm. Fig. 1(b) and (c) show the SEM micrographs of polished cut surface and the sintered joint section of scaffold, respectively. The insert image in Fig. 1(b) is taken from the top of scaffold. The Ti-Ni-Ag alloy scaffold exhibits three-dimensional networks as shown in Fig. 1(b). The metallurgical sintered joint sections formed during the sintering process as shown in Fig.1(c) reveal good fiber-fiber bonds. Fig. 1(d) shows a backscattered electron micrograph of sintered joint sections. By EDS analysis, the black-colored particles (designated by an arrow) embedded in TiNi matrix are known to be Ti_2Ni phase including Ag of 0.20 at.%. The porosity and pore size of the Ti-Ni-Ag scaffold are about 80% and 150–600 μm, respectively. The porosity in this study shows a good agreement with that of the cancellous bone possessing porosity of 50–90% [21], which can imitate cancellous bone in structure and provide space for cell and protein delivery. It is found that the pore size of scaffold should be larger than 100 μm for the successful supply of nutrients and oxygen [22]. As reported by Itin et al. [23], the size of pores varying from 100 to 500 μm was optimal for new bone ingrowth. The pore in this study is very large and can meet the requirement of pore size for new bone tissue ingrowth and nutrition supply.

Fig. 2(a) shows the DSC curves of the Ti-Ni-Ag scaffold. The upper DSC curve corresponds to the sintered scaffold. A less apparent exothermic peak designated by R* followed by a clear exothermic peak appearing at 180 K designated by M* is found in cooling curve and an endothermic peak in heating curve as shown in the upper DSC curve. Partial DSC curve is shown by a dotted line where cooling is interrupted and then heated. The phase identification of the sintered scaffold was further characterized by XRD as shown in Fig. 2(b). The diffraction peaks corresponding to B2 phase are observed at 373 K. Cooling the specimen down to 203 K, diffraction peaks corresponding to R phase appear with decreasing the intensity of diffraction peaks of B2 phase. On further cooling to 153 K, the diffraction peaks corresponding to R phase disappear with appearance of diffraction peaks of B19′ martensite. Therefore, it is known that the B2 → R → B19′ martensitic transformation occurred in the sintered Ti-Ni-Ag scaffold during cooling. The less apparent exothermic peak (R*) is due to B2 → R transformation and the peak (M*) observed at 180 K is due to R → B19′ transformation. It should be pointed out that the A_f temperature of the sintered Ti-Ni-Ag scaffold is 235 K as shown in the upper DSC curve so much lower than the human body temperature (310 K), which is unfavorable for biomedical application. Thus, the sintered Ti-Ni-Ag scaffolds were annealed at 723 K for 3.6 ks for the purpose of increasing the A_f temperature. The lower DSC curve as shown in Fig. 2(a) corresponds to the annealed Ti-Ni-Ag scaffold. Clear two exothermic peaks on cooling curve and two endothermic peaks on heating curve are observed. The partial DSC curve suggests that the first cooling peak corresponds to the second heating peak. It is can be deduced that this pair of peaks would be B2 → R transformation in cooling curve and its reverse transformation in heating curve, considering the narrow temperature hysteresis between this pair of peaks (about 2 K). Therefore, B2 → R → B19′ martensitic transformation resulting in two exothermic peaks and B19′ → R → B2 reverse martensitic transformation resulting in two endothermic peaks are confirmed by the DSC measurement. As shown in the lower DSC curve in Fig. 2(a), an attractive fact is that the R → B2 reverse martensitic transformation finish temperature (A_f) is 305 K, a little lower than the temperature of human body. It has been showed that at

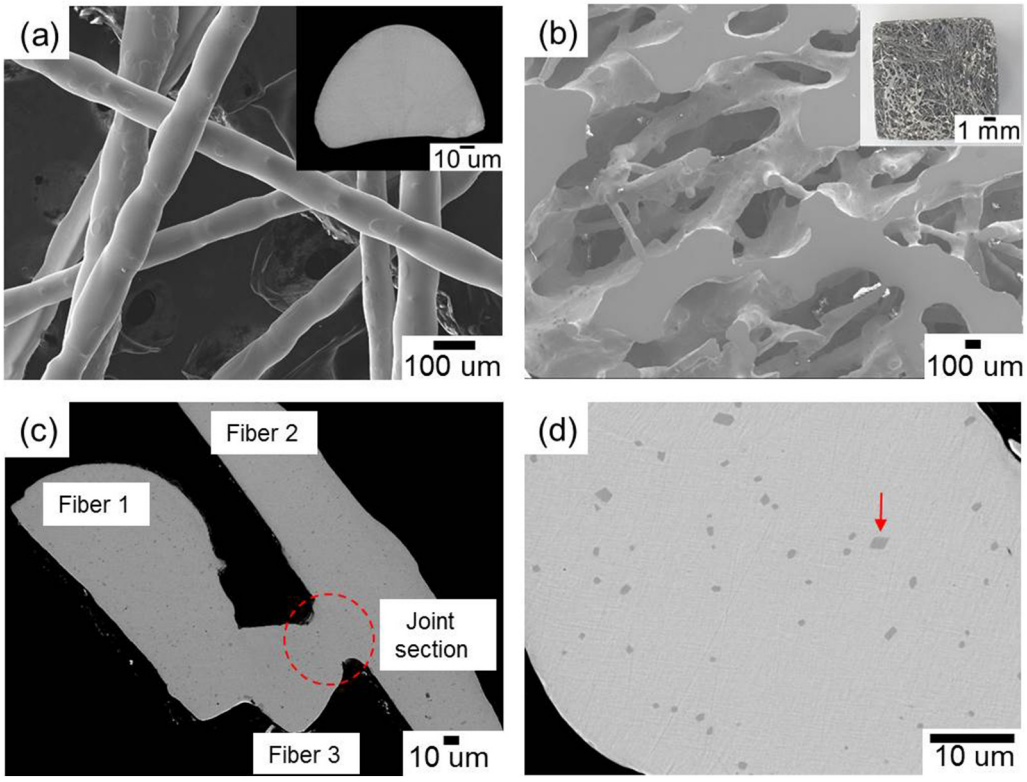

Fig. 1. SEM images showing (a) as-spun Ti-Ni-Ag fibers and (b) polished cut surface of sintered scaffold. The insert images in (a) and (b) correspond to the cross-sectional shape of fiber and the top view of scaffold, respectively. (c) and (d) are SEM image and magnified micrograph of sintered joint section, respectively.